Study of Avalanches During the Fracture of Discrete Models

Arnaud Delaplace, Stéphane Roux, Gilles Pijaudier-Cabot

HAL Id: hal-01007340

https://hal.science/hal-01007340

Submitted on 31 Jul 2017

Study of avalanches during the fracture of discrete models

A. Delaplace[a], S. Roux[b], G. Pijaudier-Cabot[c]

[a] *LMT, ENS Cachan, 61, avenue du Président Wilson, 94235 Cachan, France*
[b] *SVI, unité mixte CNRS—Saint Gobain, 39 quai Lucien Lefranc, 93303 Aubervilliers cedex, France*
[c] *R&DO, Laboratoire de Génie Civil de Nantes-Saint Nazaire, Ecole Centrale de Nantes, 1, rue de la Noe, 44321 Nantes cedex 3, France*

Fluctuations on material response due to heterogeneity are known to contain intrinsic properties of the material. Two simple discrete models are presented and the fluctuations encountered on their responses are analyzed through avalanche distributions, which represent the evolution of micro-events of degradation in the material. Both models are based on the fiber bundle model. The first one deals with the propagation of an infinite 1D crack between an elastic body and a rigid substratum. The second one deals with the rupture of a softening heterogeneous material coupled to an elastic body.

1. Introduction

The response of quasi-brittle heterogeneous materials under mechanical loads reveals an average behavior, but also fluctuations that are due to the randomness of the material micro-structure. Rupture events are a succession of micro-cracks nucleation, propagation and arrest. These events are controlled by the randomness of the distribution of material properties and also by internal correlation length scales, which are usually unknown. However, a relevant continuum model of fracture has to take into account such scales in order to avoid any discretisation sensitivity. Currently, methods that aim at exhibiting these length scales are hardly available. In this paper, we present a possible candidate. The technique is based on the study of avalanche distributions. An avalanche is a measure of the succession of micro-events (i.e. the quantity of micro-events) in the material under a given load. The analysis of the avalanche distributions has been applied to different topics (see e.g. [1,2,7]). Here, we apply this tool to the analysis of the fluctuations encountered on the responses of numerical model problems. The medium intrinsic length is extracted in both cases, which helps at understanding post-bifurcation responses.

The discrete models are based on the fiber bundle model, that allows a full analytical study of rupture. The first model is the so-called ZIP model. It represents the propagation of an infinitely long crack at the

---

interface between a rigid substratum and an elastic body. It has been studied in [8]. We will just recall the main analytical results and we will present applications for two different elastic interactions. The second model represents the failure of an heterogeneous material connected in parallel to an elastic body. It is inspired from an experimental test which has been developed in the past, in order to measure the internal length in different heterogeneous materials [3,5]. We use a hierarchical model for the elastic body. This kind of hierarchical discretisation provides a reasonable representation of the Green function in an elastic body, and it is possible to reach results on large size systems with a reasonable computation time.

2. ZIP model

This first discrete model is derived from the well-known Daniels' fiber bundle model [9]. It is an infinite set of parallel fibers clamped between a rigid substratum and an elastic body (Fig. 1). The load is an imposed displacement which moves onto a line perpendicular to the fibers axis. Fibers are elastic, with the same stiffness κ, until their displacement y reaches a random threshold y_c where they break irreversibly. We chose a distribution of random thresholds which is uniform between 0 and 1 (although it is possible to use other distributions, without any added complexity).

The model response is the variation of the global force F versus the edge displacement U. In the steady state regime, the global force F versus the location of the crack tip (which is equivalent to the number of broken fibers on the crack faces [8]) is also monitored. F is defined as the sum of the local forces f_i, where the subscript i refers to ith-fiber:

$$F = \sum_i f_i(U) \tag{1}$$

with

$$\begin{aligned} f_i &= \kappa y_i \quad \text{if } y_i \leqslant y_{c_i} \\ &= 0 \qquad \text{if } y_i > y_{c_i} \end{aligned} \tag{2}$$

This model gives a steady state regime of crack propagation which reveals many fluctuations due to the heterogeneity induced by the fibers strength (Fig. 2). It is important to emphasize that such fluctuations are really not random noise. They depend on the fibers strength, of course, but also on the redistribution of forces in the elastic body which follows each fiber rupture. This redistribution introduces some correlation in the failure process for which we would like to exhibit intrinsic properties (e.g. not dependent on the size and geometry of the system). In this paper, we shall focus on the characterisation of an internal length that gives the zone area where interactions and redistribution take place in front of the crack tip. This zone can be compared to the fracture process zone (FPZ) described by Hillerborg et al. [10], where some "bridges"
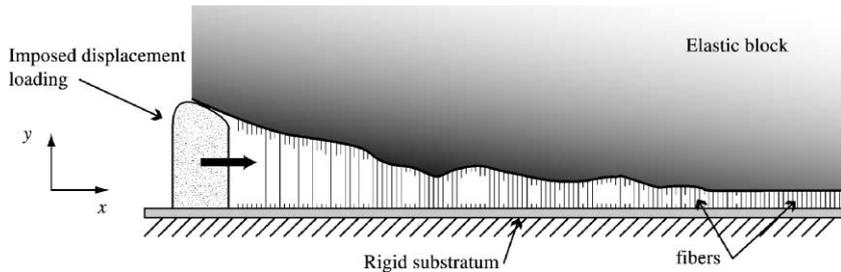
Fig. 1. A scheme of the ZIP model.
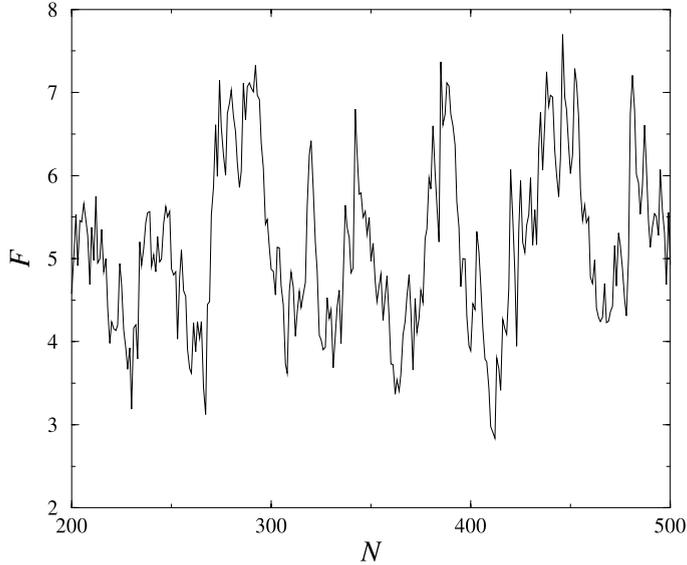
Fig. 2. A part of ZIP model response. *x*-axis represents the number of broken fibers, *y*-axis is the value of the global force *F*.

exist between the upper part and lower part of the crack. The stress field is not discontinuous across the crack tip, although with the present discrete model this aspect of the stress distribution cannot be investigated. Behind the FPZ, the crack faces are not connected; ahead of the FPZ, material is sound. In the ZIP model, we distinguish three regions that are similar to the ones described by Hillerborg. The first one is called the broken area (behind the FPZ) with broken fibers only, the second one is called the active area (the FPZ) where surviving fibers and broken ones are present and the last one is called the safe area (ahead of the FPZ) where no fibers are broken.

The size of the FPZ is an important intrinsic property of the material. Knowing this size is crucial when dealing with scale effects e.g. with enriched models for continuum failure (see [11,15,16]). With such models, the internal length controls the width and length of the FPZ. In boundary value problems, the variation of the ratio of the size of the FPZ to the size of the structure yield results that are size dependent. This size effect observed experimentally cannot be captured with continuum models where an internal length is not inserted in the formulation (in gradient or integral nonlocal formulations, or in the form of a cohesive crack with a FPZ). Unfortunately, this length is not easily obtained experimentally. On the simple numerical models considered in this contribution, we are going to show that because the fluctuations encountered on the response depend on internal material properties, the analysis of avalanche distribution provides this internal length, or at least the size of the FPZ. In order to better understand the results, we recall first the main conclusions obtained for the ZIP model.

2.1. Analytical results

These results are obtained from a simplified version of the ZIP model. In this part, we choose an imposed displacement profile for the elastic body. It allows to perform a complete statistical analysis of the problem (for a detailed derivation of the results in this section, see [8]). The chosen profile is given by

$$y(x) = \exp\left(\frac{(U(t) - x)}{\xi}\right) \tag{3}$$

where the parameter ξ is considered as a fixed parameter of the model. This simplified expression captures the main features of the deflection of a beam which is connected on a rigid substratum through a damageable interface. Because we focus on the fluctuations of the steady state response of the system, we deal with the variance of $dF = F(U + \Delta U) - F(U)$. F is the sum of independent statistical variables, hence dF is obtained from the sum of df_i. After some mathematical manipulations, the following expression is derived:

$$\langle dF^2 \rangle = (1 - \exp(-\Delta U / \xi))\sigma^2(F) \tag{4}$$

where $\sigma^2(F)$ is the total force variance. The interpretation of this expression is the key point to understand correlations along the response model: over the length scale ξ (ΔU lower than ξ), F behaves as a random walk and there exists correlations between the fiber responses (i.e. their rupture). For larger distances ($\Delta U > \xi$), the fluctuations are uncorrelated and the fibers break randomly.

The distribution of avalanches is well-known for this kind of fluctuating signal [17]. For an uncorrelated signal, the distribution is a simple power law $p_1(\Delta) = \Delta^{-2}$. For a random walk, the distribution is also a power law but with an exponent $-3/2$. In the present model problem, the same type of result should be expected, because over a length that is lower than the FPZ size (in the order of ξ), fluctuations reveals correlation. In the ZIP model, the analysis of the distribution of the avalanches of size lower than ξ should give a power law of $-3/2$. The analysis of the distribution of avalanches of size greater than ξ should give a power law with an exponent -2 because the response is no more correlated.

2.2. Numerical results

In this section, we present the distributions of avalanches obtained from two kind of enhanced ZIP models. In the first one, a beam is connected to the substratum through the damageable interface. In the second one, it is a 2D semi-infinite elastic body which is connected to the substratum through the same interface (Fig. 1). The infinite boundary condition at the opposite side of the edge is guaranteed by a particular elastic element: this element captures the behavior of an infinite elastic body connected to a rigid substratum through an infinite set of intact fibers. For the first case of a beam, the property of this element (called A) is depicted in Fig. 3.

2.2.1. Elastic beam

The problem is solved by considering two degrees of freedom (vertical displacement and rotation) for each point of the beam connected to a fiber. For two neighboring points i and j, it corresponds to nodal degrees of freedom v_i, θ_i, v_j, θ_j. Under the assumption of an Euler–Bernoulli beam, the stiffness matrix is given by
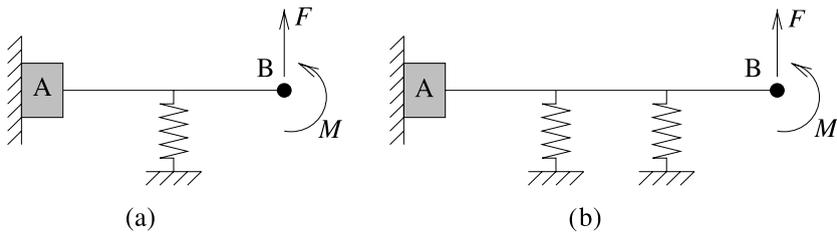
Fig. 3. Features of element A ensure that the vertical displacement and rotation of point B under loading force F and torque M are equal in both cases (a) and (b).

$$\mathbf{K} = \frac{EI}{l^3} \begin{bmatrix} 12 & 6l & -12 & 6l \\ 6l & 4l^2 & -6l & 2l^2 \\ -12 & -6l & 12 & -6l \\ 6l & 2l^2 & -6l & 4l^2 \end{bmatrix} \tag{5}$$

where E is the elastic modulus, I the moment of inertia of the cross-section and l the beam length between the two points. The size of the active area (or the FPZ) is a priori unknown. It depends on the ratio between the fibers stiffness κ and beam stiffness EI. We plot in Fig. 4 two avalanche distributions where the beam stiffness has been changed only: the ratios EI/κ are chosen to be 1×10^3 and 2×10^3 (respectively crosses and circles on the figure). The two expected distributions are obtained, with a cross-over that gives the size of the FPZ.

2.2.2. Semi-infinite elastic body

In this second case, the beam is replaced by a semi-infinite elastic body. At the boundary of the elastic solid which is connected to the fibers, one degree of freedom (vertical displacement) is imposed. In order to solve the problem, we use the Green function [14] that provides the displacement y along the elastic body due to a force f applied at distance l of the point where the displacement is measured:

$$y(l) = \frac{2f}{\pi E} \log \frac{\lambda}{|l|} - \frac{(1+v)}{\pi E} f \tag{6}$$

E and v are the Young modulus and the Poisson ratio of the elastic body. λ is a constant that corresponds to a zero vertical displacement. The crack propagation in this model is similar to that of the previous one, except that interactions inside the FPZ depend on Green functions instead of being the solution of a beam
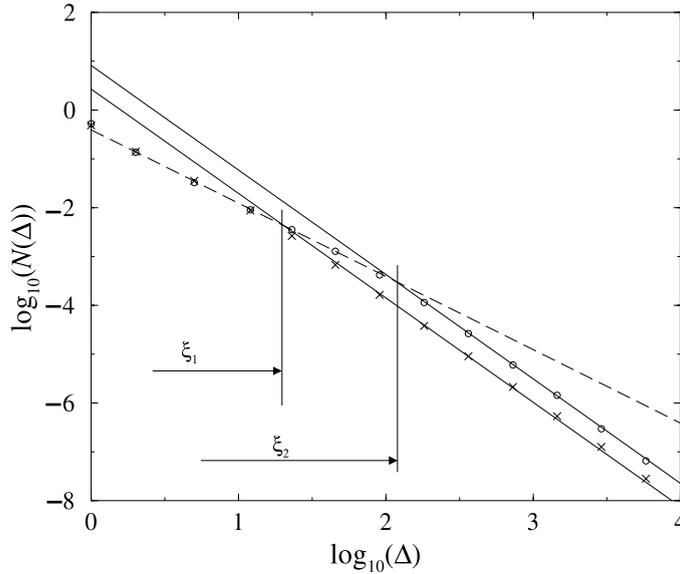
Fig. 4. Avalanche distributions for two beam stiffnesses. They exhibit two power-laws, the first one with an exponent $\tau_1 = 1.50 \pm 0.05$ (– – –) and the second one with an exponent $\tau_2 = 2.05 \pm 0.10$ (—). The cross-over between the two slopes gives the size of the active area (ξ_1 and ξ_2 on the figure).
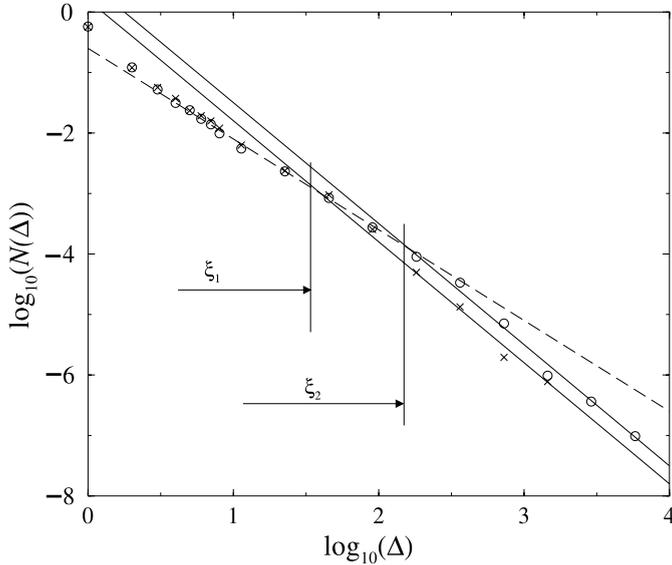
Fig. 5. Avalanche distributions for two elastic bodies stiffnesses. They exhibit the expected two power-laws. The cross-overs (called ξ_1 and ξ_2) give the length of the FPZ size.

problem. The length of the FPZ is again not known. Then, we compute the distribution of avalanches in order to find this length, which corresponds to the cutoff between the correlated signal and the uncorrelated one. Two distributions are plotted in Fig. 5 for two elastic moduli of the semi-infinite block. We find, as expected, the two regimes with the cutoff which corresponds to the size of the FPZ.

2.3. Comments on the ZIP model

We have shown above that the distribution of avalanches contains useful information on the correlation of fracture events in heterogeneous media. The above analyses show, in particular, that it is possible to extract the size of the FPZ from the distribution of avalanches. It is important to emphasize that this kind of analysis could not be carried out if the response would be smoothed, for instance if the average steady state response would be considered only, without the fluctuations. A continuous response, however, could be seen as the limit of such an average response for a model with an infinite number of fibers. It is not the case: the response of the discrete model is not differentiable. Upon taking the limit of a discrete model to the infinite size, it is found that the response is still not differentiable. It is not in agreement with the traditional assumption of continuum models. Simply, it shows that the smoothing that is involved in continuum models, for which the response is differentiable, erases some features of the way local failure develops in the FPZ.

The results obtained with the two ZIP models could be extended to other similar models. For instance, if we consider a 2D crack propagation (with a set of parallel fibers in x and z directions), the analysis of the distribution of avalanches would give a cutoff that is proportional to the area of the FPZ. Finally, such a technique should be applied to experimental studies of in-plane crack propagation in a heterogeneous material. In the next part, we discuss another model which represents the rupture of an heterogeneous material coupled in parallel to an elastic body. Again, the avalanche distributions will be able to reveal information on heterogeneity effects.

3. Hierarchical model

Dealing with the post-peak behavior of quasi-brittle heterogeneous material under tension has ever been delicate. In the post-peak regime, the response of the specimen is very much unstable. Strain localisation occurs, which prevents a direct measurement of the material response in tension. Different experimental attempts have been proposed in order to stabilize the specimen response and to prevent, as much as possible, strain localisation to occur [12,13]. One popular test is the so-called PIED test developed by Berthaud et al. [3] from an original idea of l'Hermite [4] and Bazant and Pijaudier-Cabot [5]. The idea is to apply a uniform state of uniaxial tension on the specimen through parallel elastic bars glued on the material. For instance, aluminum bars are chosen for tests on concrete (Fig. 6). Micro-cracks are expected to appear all over the material, without the occurrence of a single macro-crack propagation. The model discussed in this section mimics this experiment. The material to be tested (on which the elastic fibers are glued) is described by a set of fiber bundle models.

The aim of this device is to avoid the occurrence of a macro-crack. It could be easily reached by considering a large stiffness for the elastic body with respect to the material stiffness. But the larger the elastic stiffness is, the more difficult it is to obtain the material response accurately. On several tests, macro-cracks and so nonuniform strain states have been detected. In this case, the specimen response is not a function of the material tested only. For instance, it has been shown [6] that a macro-crack could lead to a debonding at the material–bars interface, and the assumptions used to extract material behavior are no longer verified. One of the problem is that macro-cracks are not directly visible after the test because the elastic bars tend to close them upon unloading. The only way to reveal the macro-crack is to cut the sample.

We are going to study the response of a specimen similar to that of the PIED test, described by a theoretical model in such a way that the occurrence of a nonhomogeneous strain field can be detected. This can be done again by studying the distribution of avalanches. Before showing some results, we will recall some of the useful properties of the distributions of avalanches, based on the ones observed with ZIP model.

3.1. Theoretical model

We use here a hierarchical discretisation of the specimen. Fig. 7 shows the discretisation (also called generation) at levels 1–3. The most important feature the model has to verify is that the stiffness of the elastic body has to be independent of the discretisation level [7]. This aim is reached if the parallel springs in the hierarchical discretisation have half the global stiffness k.

We may now write the recurrence relations that control the system. They are obtained by writing the force–displacement response of a system at generation (n) from the responses of two systems at generation ($n - 1$). The displacement is simply:
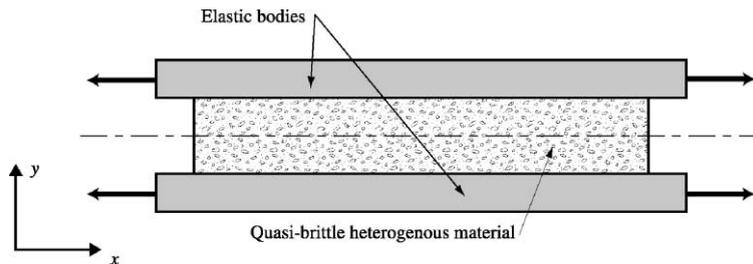
Fig. 6. A scheme of a PIED experimental setup.
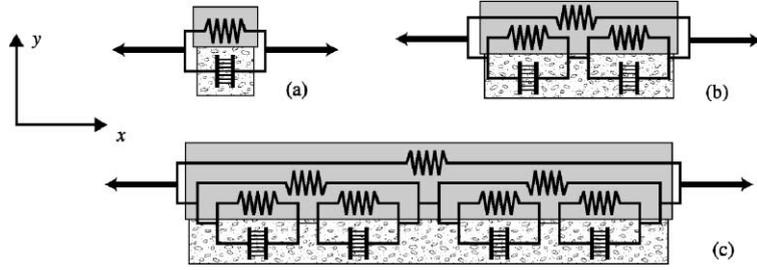
Fig. 7. The hierarchical decomposition for systems of generation 1 (a), 2 (b) and 3 (c).

$$U^{(n)} = U_1^{(n-1)} + U_2^{(n-1)} \tag{7}$$

and the force is:

$$F^{(n)} = F^{(n-1)} + \frac{k}{2}(U_1^{(n-1)} + U_2^{(n-1)}) \tag{8}$$

If we consider a homogeneous response for the material (i.e. $U_1^{(n-1)} = U_2^{(n-1)}$) then the global response of the model from the response of the system at generation 1 is:

$$F^{(n)} = F^{(1)} + k(2^{n-1} - 1)U^{(1)} \tag{9}$$

$$U^{(n)} = 2^{n-1}U^{(1)} \tag{10}$$

3.2. Bifurcation analysis

The aim of the experimental device depicted in Fig. 6 is to obtain a uniform distribution of strain and damage in the material which is tested by a control of the displacement field on the lateral faces of the specimen. The bars are placed so that bifurcation and strain localisation is prevented, as much as possible. In order to check this, let us make a bifurcation study of the model. For this, we need to assume that the material to be tested follows a strain softening response. We chose here the mean behavior of a Daniels' model with a uniform probability distribution for the fiber thresholds between 0 and 1. This force–displacement behavior is:

$$f = \kappa u(1 - u) \tag{11}$$

where κ is the initial stiffness, and u is the normalized displacement which varies between 0 and 1. The recurrence relations start from the response of a system at generation (1):

$$U^{(1)} = u \quad \text{and} \quad F^{(1)} = \kappa u(1 - u) + ku \tag{12}$$

The unstable condition is reached when:

$$\frac{dF^{(n)}}{dU^{(n)}} = 0 \quad \text{or} \quad u = \frac{2^{n-1}k + \kappa}{2\kappa} \tag{13}$$

From the last equation, we can see that if the unstable condition is not reached for the first generation system, the condition will never be reached. Because $u \in [0; 1]$,

$$k > \kappa \tag{14}$$

is a sufficient condition to have a stable solution. Of course, this kind of analysis could be done because the material response is entirely defined a priori.

If the unstable condition is reached during a test, the material response derived from a direct interpretation of the test data, which assumes that the material and the bars form a parallel system with a homogeneous strain, will not be the real one. The difficulty is that it is quite impossible to know if this state is reached: if a bifurcation occurs, a macro-crack will propagate suddenly, and the system will move to an other stable configuration. The loading could be a succession of such unstable events, as the global response looks like a stable one. For this discrete model, however, the response still reveals some fluctuations due to randomness of fibers thresholds. Same as for the ZIP model, the distribution of avalanches should provide some informations on failure process.

3.3. Avalanches

Before dealing with distributions of avalanches, let us describe first the failure process. At the beginning of the loading, the weakest fibers break randomly in the sample, because of the stress field is homogeneous. When the peak load is reached, the system failure is the result of a competition between two processes:

- The first one follows the previous one, i.e. a random locations of broken fibers.
- The second one corresponds to a local redistribution regime. In this case, bifurcation can occur locally and leads to a stress redistribution in the neighborhood of the region where local failure occurs, due to the elastic bars. Then, the stress homogeneity is no longer guaranteed.

If the aim of the test is to capture the global response of the heterogeneous material under a homogeneous strain, the first failure process should develop only. This kind of regime, without redistribution, is similar to a random signal that gives a well-known power law of the distributions of avalanches. If the system follows the second failure process, the distribution of avalanches will exhibit another law which is not known analytically (note that for simple models with local load sharing, it could be obtained analytically [18]). We present now computations of the distribution of avalanches for different systems with different stiffnesses of the elastic bars.

3.3.1. Numerical results

We chose a set of fibers with a uniform distribution between 0 and 1 for the thresholds. In this particular case, we know from Eq. (14) which stiffness corresponds to the transition between a localized failure process and a full random failure. Two distributions of avalanches are presented. The first one corresponds to $k = 2\kappa$. As expected, the distribution follows a power law with an exponent -2 (Fig. 8). The location of the successive broken fibers is shown in Fig. 9 for a 7-generation model with 100 fibers in each bundle. The failure is homogeneous all over the loading. The second distribution corresponds to $k = 0.2\kappa$. In this second case, the distribution of avalanches does not follow the power law with an exponent -2, and diverges from this behavior. As explained before, at the beginning of the failure, the fibers break randomly. This regime corresponds to the power law of -2. After the peak load, the failure process is controlled by local redistributions and the distribution of avalanches becomes biased compared to that of Fig. 10. The failure is no longer homogeneously distributed (Fig. 11). Note that the computed distribution is an average between two regimes that occur *successively*, contrary to the distribution obtained with the ZIP model which reveals two regimes which occur simultaneously. This feature is shown in Fig. 12. The distribution of avalanches of a 6-generation system with 1000 fibers per bundle is plotted at different steps of the loading. Before bifurcation, the distribution remains a straight line in a log–log plot. After localisation, distribution diverges from this
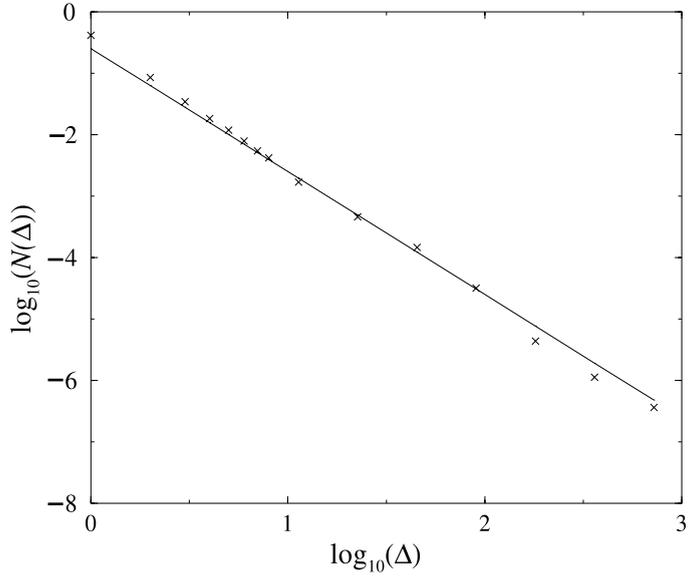
Fig. 8. The avalanche distribution of a hierarchical model of generation 4, with 1000 fibers per bundle. The chosen stiffness is $k = 2\kappa$. The dashed line is a guide for the eyes and has a slope of -2.
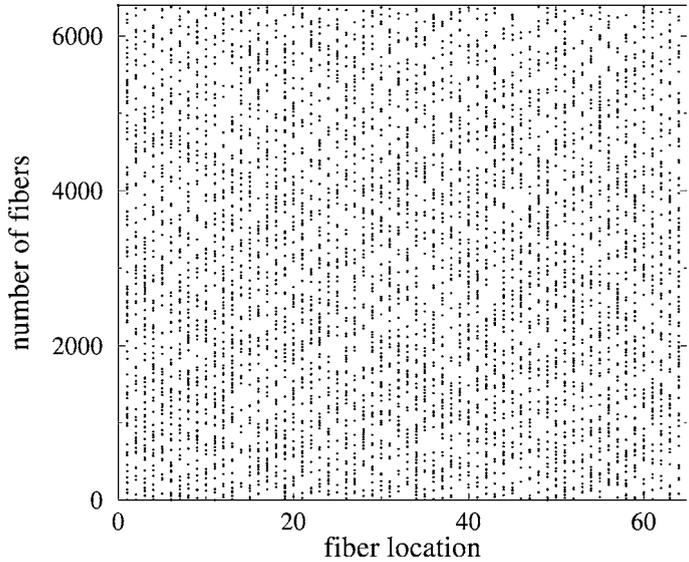
Fig. 9. Location of fibers during the failure. y-axis represents the succession of the broken fibers during the loading, x-axis represents the position of the broken fiber. Fibers break homogeneously during the loading. Each point is the failure of one fiber. Fibers break homogeneously during the loading.

line. These results show that through a simple analysis of the fluctuations encountered on the response of the model numerical problem, it becomes possible to check if bifurcation occurs during test. This approach
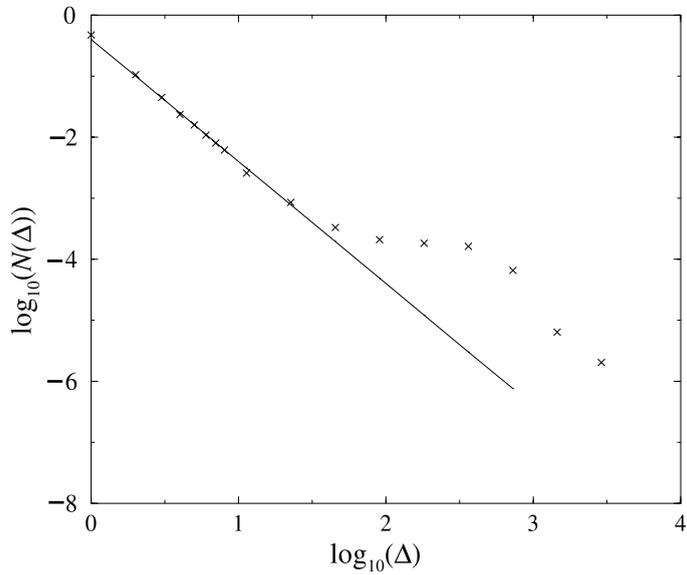
Fig. 10. The avalanche distribution of a hierarchical model of generation 4, with 1000 fibers per bundle. The chosen stiffness is $k = 0.2\kappa$. As expected, the distribution does not follow the slope of −2.
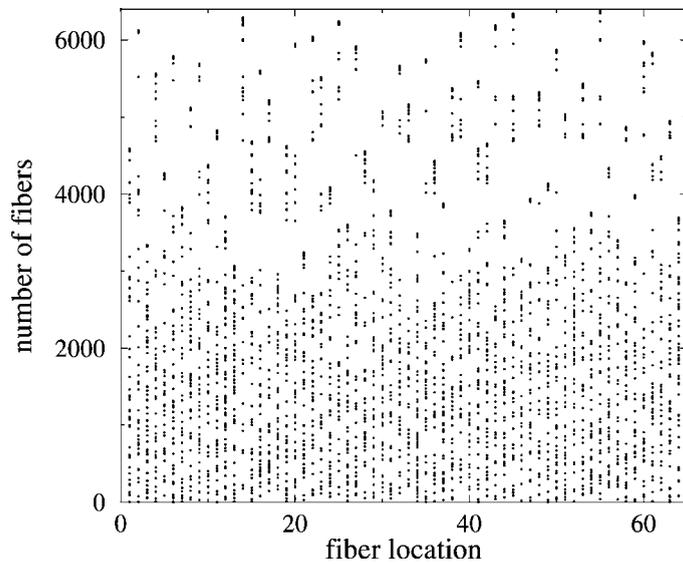
Fig. 11. In the case $k < \kappa$, the localisation of broken fibers into a bundle could be seen at the end of the loading. In the beginning of the loading (before bifurcation), no localisation occurs.

is expected to be used on experimental test, where acoustic emissions, same as avalanches, are micro-events occurring in the material during failure. The analysis of their distributions should give relevant information on the failure process.
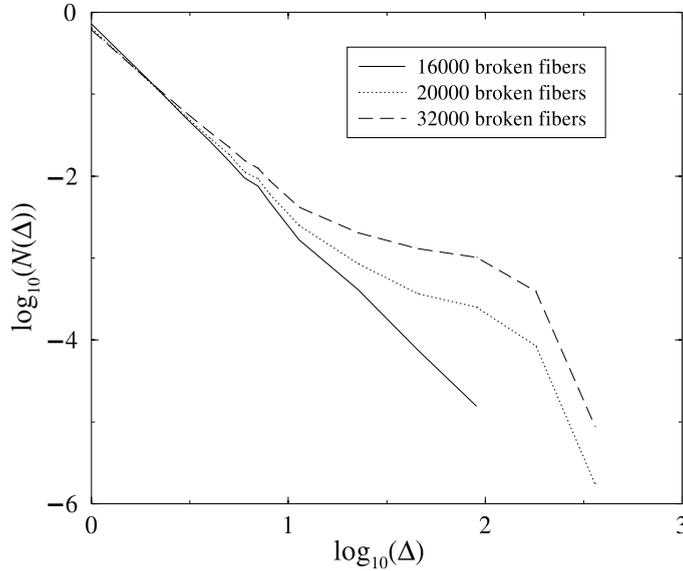
Fig. 12. Evolution of avalanche distribution for a hierarchical model of generation 6 with 1000 fibers per bundle. The distribution is plotted after 16 000 broken fibers (before bifurcation), 20 000 and 32 000 (after bifurcation).

4. Conclusion

Several discrete numerical models which reveal fluctuations of their response have been discussed. These fluctuations are close to the ones that are encountered in the experimental responses of quasi-brittle material subjected to tensile loads. In a continuum mechanics approach, the material response is represented as a smooth one, loosing some important features such as fluctuations of the applied load. Taking into account the variability of the response provides some extra information on the failure process. This paper underlines the idea that fluctuations on material response are really relevant for a better understanding of the behavior of quasi-brittle materials.

Inspired from the ZIP model, the first two model problems deal with the propagation of an infinite in-plane crack at the interface between an elastic body and a rigid substratum. This kind of crack propagation are known to exhibit a FPZ in front of the crack tip, whose size is proportional to an internal length. A similar one-dimensional zone is developed at the crack tip in the ZIP model, where surviving and broken fibers are present. This zone is characterized by a length that is a priori unknown in the model. It can be looked at as a simplistic description of a FPZ. The distributions of avalanches show that this length could be obtained by considering two regimes: one regime where the local failures are correlated, and the other one which is close to random.

The second model mimics an experimental test aimed at controlling the damage process in the material. It is intended to prevent strain and damage localisation to occur with the help of restraining bars glued on the faces of the specimen. The distribution of avalanches helps at revealing whether it is indeed what occurs during the experiment or not. If there is no redistribution, the fibers break randomly in the media, and lead to a well-known distribution of the avalanches described with of a power-law with an exponent of −2. If redistribution occurs, the distribution of avalanches diverges from this power law. Therefore, a full analysis of the experimental response, including its fluctuations, may provide some information on the homogeneity of the strain distribution inside the specimen.

References

[1] Paczuski M, Maslov S, Bak P. Avalanche dynamics in evolution growth and depinning models. Phys Rev E 1996;53:414–43.

[2] Hansen A, Hemmer P. Criticality in fracture: the burst distribution, Theoretical Physics Seminar in Trondheim, Norway, 1994.

[3] Berthaud Y, Ringot E, Fokwa D. A test for delaying localisation in tension: experimental investigation. Cement Concrete Res 1991;21:928–40.

[4] l'Hermite R. Volume changes in concrete. In: Proceedings of the 4th International Symposium on the Chemistry Cement, Washington, BC, 1960. p. 659–702.

[5] Bazant ZP, Pijaudier-Cabot G. Measurement of the characteristic length of non-local continuum. J Engng Mech 1989;115(4): 755–67.

[6] Boudon-Cussac D, Hild F, Pijaudier-Cabot G. Tensile damage in concrete: analysis of experimental technique. J Engng Mech 1999;125(8):906–13.

[7] Delaplace A, Roux S, Pijaudier-Cabot G. 'Damage cascade' in a softening interface. Int J Solids Struct 1999;36:1403–26.

[8] Delaplace A, Roux S, Pijaudier-Cabot G. Avalanche statistics of interface crack propagation in fiber bundle model: characterization of cohesive crack. J Engng Mech 2001;127(7):636–52.

[9] Daniels HE. The statistical theory of the strength of bundles of threads. Proceedings of the Royal Society London A 1945;183:405–35.

[10] Hillerborg A, Modeer M, Petersson PE. Analysis of crack formation and crack growth in concrete by means of fracture mechanics and finite elements. Cement Concrete Res 1976;6:773–82.

[11] Le Bellego C, Dube JF, Pijaudier-Cabot G, Gerard B. Calibration of non local damage model from size effect tests. Eur J Mech A/Solids, submitted for publication.

[12] Mazars J, Berthaud Y, Ramtani S. The unilateral behavior of damage concrete. Engng Fract Mech 1990;35(4–5):629–35.

[13] Mazars J, Ramtani S, Berthaud Y. An experimental procedure to delocalize tensile failure and to identify the unilateral effect of distributed damage. In: Mazars J, Bazant ZP, editors. Cracking and damage. Elsevier Applied Sciences; 1988.

[14] Timoshenko S. *Théorie de l'élasticité*, Librairie Polytechnique, Paris and Liège, 1948.

[15] Peerlings RH, de Borst R, Brekelmans WAM, Geers MGD. Gradient enhanced modeling of concrete fracture. Int J Num Meth Engng 1996;39:3391–403.

[16] Pijaudier-Cabot G, Bazant ZP. Non local damage theory. J Engng Mech, ASCE 1987;113:1512–33.

[17] Hemmer PC, Hansen A. The distribution of simultaneous fiber failures in fiber bundles. J Appl Mech 1992;59:909–14.

[18] Kloster M, Hansen A, Hemmer PC. Burst avalanches in solvable models of fibrous materials. Phys Rev E 1997;56.